Correlating dopant distributions and electrical properties of boron-doped silicon nanowires

Ruth A. Schlitz, Daniel E. Perea, Jessica L. Lensch-Falk, Eric R. Hemesath, and Lincoln J. Lauhon[a)]

Department of Materials Science and Engineering, Northwestern University, 2220 Campus Dr., Evanston, Illinois 60208, USA

(Received 22 April 2009; accepted 23 September 2009; published online 19 October 2009)

Quantitative nonuniform radial doping profiles in vapor liquid solid grown boron-doped silicon nanowires are correlated with axial variations in electrical properties. Boron concentrations measured by atom probe tomography are lower for the core material grown from a gold catalyst than for material deposited on the nanowire surface. Transistors fabricated along a single nanowire exhibit a transition from nonlinear contact-dominated behavior to linear behavior with increasing thickness of the dopant-enriched surface layer. Simple models confirm that the surface is doped to a level that enables the contact resistance to become comparable to the channel resistance, suggesting that unintentional surface doping may play a role in lowering contact resistances in some nanowire devices. © *2009 American Institute of Physics*. [doi:10.1063/1.3250431]

Vapor-liquid-solid (VLS) grown semiconductor nanowires have been incorporated into a variety of nanoscale devices,[1–5] and recent improvements in device uniformity over large areas[1,6,7] indicate substantial promise for nanowire electronics. While much of the reported work assumes that nanowires grow exclusively in the axial direction, nonselective vapor-solid (VS) deposition on the nanowire surface can occur simultaneously with VLS nanowire growth, leading to a tapered morphology and possible nonuniformities in structure and composition. Considering that dopant incorporation rates via VS and VLS growth may differ,[8] gradients in carrier concentration may arise along the length of the nanowire. Dopant-enriched VS deposition has previously been observed by atom probe tomography of phosphorous-doped Ge nanowires[8,9] and Raman microscopy of boron-doped silicon.[10] In general, the device properties are highly dependent on the amount of uncatalyzed VS deposition.[11]

Here we correlate the electrical characteristics of boron-doped silicon nanowire field effect transistors (NWFETs) with the boron distribution using atom probe tomography. We find that the device characteristics are sensitive to radial and longitudinal inhomogeneities in boron concentration arising from unintentional VS deposition. Near the nanowire tip, devices are rectifying and dominated by Schottky barriers at the contacts; near the base, devices become Ohmic, indicating that the contact resistance has decreased to the order of the channel resistance. This behavior is consistent with the sensitivity of the tunneling probability through the Schottky barriers to the dopant concentration for the measured doping values.

Boron-doped silicon nanowires catalyzed by gold nanoparticles were grown in a hot-walled chemical vapor deposition chamber via the VLS mechanism using silane (SiH_4) and diborane (B_2H_6) in a Si:B ratio of 3000:1 at $T=440$ °C and $P=40$ Torr. The nanowires had an average diameter of 20 nm near the catalyst tip increasing to 30 nm at the base. Under these growth conditions, gold does not diffuse away from the catalyst particle, so the taper arises solely from VS deposition along the wire during growth. Given an average length of 12 μm, the diameter change corresponds to a VLS:VS growth rate ratio of 2400:1, as depicted schematically in Fig. 1(a). Nanowires were removed from the growth substrate and suspended in isopropanol using ultrasonication before deposition onto degenerately doped silicon substrates with 200 nm of silicon nitride as a back gate dielectric. Ni contacts (~40 nm thick) were fabricated on individual nanowires using electron beam lithography to create four NWFET devices of equal channel lengths. Intruded θ-Ni_2Si contacts were formed by rapidly annealing for 30 s at 450 °C in forming gas (95% N, 5% H), similar to processes reported elsewhere.[12–14] An atomic force microscopy (AFM) topograph of a completed device is shown in Fig. 1(b); the average channel length is 1.04 μm, with the in-

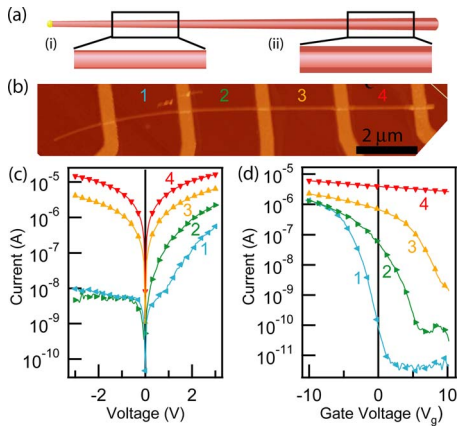

FIG. 1. (Color online) (a) Schematic of a VLS nanowire that is tapered due to surface vapor-solid (VS) growth of doped material during synthesis. (b) AFM image of four back-gated NWFETs along a nanowire that has accumulated 5 nm of VS coating at the nanowire base. The nanowire tip ($d_{tip}=24$ nm) is at left; devices are numbered 1–4 from tip to base ($d_{base}=32$ nm). (c) *I-V* data for each device. Devices 1 and 2 near the tip are rectifying, while devices 3 and 4 near the base are Ohmic in character. (d) Gate response for each device ($I_{ds}=1$ V). Increasing off-currents toward the base are consistent with a core of moderately doped material surrounded by a more heavily doped shell that is not fully depleted by the back gate.

[a)]Author to whom correspondence should be addressed. Electronic mail: lauhon@northwestern.edu.

truded silicide extending 530 nm on average from the Ni contacts. Given the degree of taper, the channel of each device, from 1–4, contains approximately 1 nm of additional VS shell material.

Current-voltage characteristics [Fig. 1(c)] reveal that devices near the tip are rectifying and less conductive than devices near the base, which are Ohmic in character. Similar results were observed for eight devices made from four different nanowires.[15] In Fig. 1(c), the contact closer to the nanowire tip was biased for each respective device. The consistent direction of rectification for devices 1 and 2 indicates that the Schottky barrier closer to the nanowire tip (for each respective device) is wider, that is, the largest current is observed when this junction is forward biased. These results suggest the presence of a gradient in carrier concentration along the length of the nanowire altering the width of the Schottky barrier; this hypothesis is supported by the decreasing transconductance from the tip to the base [Fig. 1(d)]. A gradient in carrier concentration along the length of the nanowire arises from enhanced incorporation of dopants on the nanowire surface by the VS deposition, as shown below. Indeed, the variations in off-currents with position in Fig. 1(d) are consistent with the presence of a heavily doped shell that only weakly responds to an applied potential.

Atom probe (APT) tomography was recently established as a means to quantitatively map the three-dimensional (3D) dopant distribution in Si (Ref. 9) and Ge nanowires.[8,9] For the present study, we utilized *p*-Si/Ge core/shell and Ge/*p*-Si core/shell radial heterostructures to measure the B concentration in the Si VLS core and VS shell, respectively. Separate, freestanding nanowires for APT analysis were grown atop Si or Si/Ge nanocones under similar conditions to those described above using 30 nm catalysts; additional details are provided in the supplement.[15] In APT, the nanowire is analyzed from the tip downwards; a sample portion of the reconstructed 3D data is shown in both end-on [Fig. 2(a)] and edge-on [Fig. 2(b)] views. The proximity histogram in Fig. 2(c), which plots the composition as a function of radial distance from the Si–Ge interface, is suggestive of an enhanced concentration of B at the nanowire surface.[16] Because the APT analysis is performed at the very tip of the nanowire, the accumulated VS material here is not sufficient to make this claim. To better compare VLS and VS doping rates, thicker VS shells of *p*-Si were grown on Ge nanowire cores under the same conditions used to grow the *p*-Si nanowires. Compositional analysis of volumes within the VLS-grown core for five different nanowires reveal an average dopant concentration of $N_{VLS}=8\pm2\times10^{18}$ cm^{-3}, while analysis of material grown by the VS growth mechanism reveals an average dopant concentration of $N_{VS}=2\pm0.4\times10^{19}$ cm^{-3} [Fig. 2(d)]. It is unlikely that the observed dopant distributions are influenced by boron diffusion, as the bulk diffusivity predicts that boron atoms diffuse <1 nm during nanowire growth and the subsequent shell deposition.[17] The quantitative measurement of boron concentrations allows us to correlate nanowire compositional inhomogeneities with variations in the device characteristics, providing a more detailed understanding of the material factors that control NWFET performance.

When the boron-enriched VS shell reaches a critical thickness, devices transition from rectifying, Schottky contact-dominated behavior to ohmic behavior. Figure 3(a) compares the differential resistance dV/dI at 0 V_{DS}, where

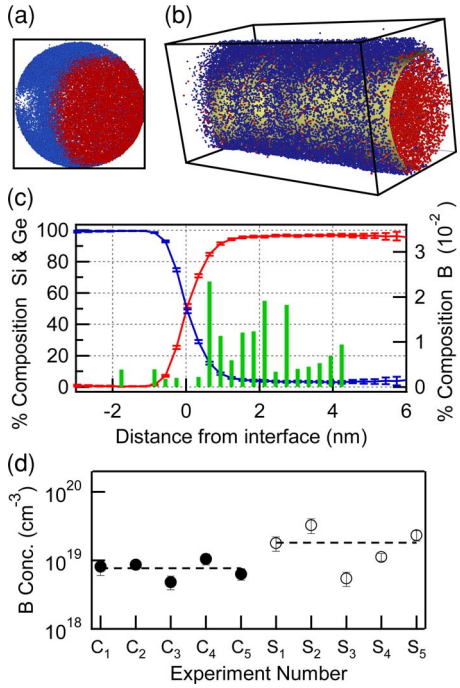

FIG. 2. (Color online) (a) End-on and (b) side-on views of a 3D reconstruction of a B-doped Si core (red) and i-Ge shell (blue) nanowire. The isoconcentration surface for 50% Si, shown in gold, is used as a reference point for the radial composition profile shown in (c). Dimensions are 23×23 nm^2 and $23\times23\times45$ nm^3 for (a) and (b), respectively. (c) Radial composition profile with B concentration indicated by the green bars. The number of counts per bin becomes smaller farther from the interface; only bins with sufficient counts are shown. (d) B concentrations for several nanowires extracted from the core region (VLS, filled circles), and from doped Si shells on Ge nanowires (VS, open circles). The dotted line indicates the gas-phase B:Si ratio during synthesis.

contact resistance dominates for rectifying devices, to dV/dI at 3 V_{DS}, where the entire device behaves as a resistor. The more rectifying contact in a given device is measured in forward bias, implying that the less resistive Schottky contact is in reverse bias. Near the nanowire tip (device 1), where there is less VS deposition, $dV/dI|_{0\ V}$ is much greater than $dV/dI|_{3\ V}$, consistent with the observation that devices at the nanowire tip are rectifying, and thus dominated by the contact resistance. In contrast, the low bias and high bias differential resistance are nearly the same at the nanowire base (device 4), consistent with an Ohmic resistance $R=V/I$ arising from both contacts and channel. The abrupt decrease of $dV/dI|_{0\ V}$ compared with $dV/dI|_{3\ V}$ between ~2 and 3 nm of overcoating (devices 2 and 3, respectively) suggests that a minimum thickness of B-doped material is required to produce Ohmic contacts. This is consistent with a recent report describing the increase in ionization energy, and thus deactivation, of dopants near the surface of a nanowire.[18]

Simple models of contact and channel resistances show that in the doping range measured by APT, the device contacts are much more sensitive to small changes in doping than the channel. The solid line in Fig. 3(b) plots the total resistance[19] of two 24 nm circular *p*-Si–Ni_2Si Schottky barrier contacts of height 0.4 eV using the Varahramyan–Verret model. While the Varahramyan–Verret model was derived for Ti_2Si contacts, and the Schottky barrier may be modified by the nanoscale geometry, the exponential variation of barrier width (and hence resistance) with dopant density is the

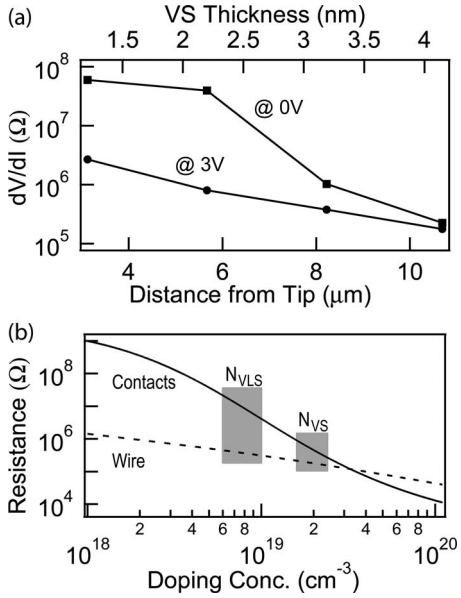

FIG. 3. (a) Comparison of two-probe differential resistances. $dV/dI|_{3\ \mathrm{V}}$ (circles) indicates a gradually decreasing channel resistance with increasing VS overcoating, whereas the $dV/dI|_{0\ \mathrm{V}}$ (squares) indicates a dramatic decrease in contact resistance between 2 and 3 nm of VS coating. (b) Approximate models of contact and channel resistances using dimensions from device 1(d=24 nm, l_{ch}=1.04 μm). The solid curve plots the contact resistance (Varahramyan–Verret model) (Ref. 17) for two Schottky contacts to p-Si with a 0.4eV barrier height. The dashed line plots the Si nanowire resistance assuming a bulklike mobility appropriate to the doping level (Caughey–Thomas model). The gray boxes indicate the ranges of B concentrations for the VLS core and VS shell measured with APT.

main qualitative feature of interest. The model provides a reasonable starting point for comparison with the qualitative features of the electrical transport data. The dashed line plots the resistance of a 24 nm diameter Si nanowire 1.04 μm in length assuming a bulklike mobility appropriate to the doping level (Caughey–Thomas model with Klaassen coefficients).[20,21] At dopant concentrations measured by APT for the VLS core material, the contact resistance is approximately two orders of magnitude larger than the resistance of the nanowire channel. For dopant concentrations on the order of those measured in the VS shell, the contact and channel resistances are of the same order of magnitude. If the measured field effect mobility of device 3 (μ=15 cm^2/V s) is used, the crossing point of the calculated contact and wire resistances shifts slightly to the left, indicating comparable contact and channel resistances. These simple estimates of the relative importance of contact and channel resistances explain (1) the abrupt drop in $dV/dI|_{0\ \mathrm{V}}$ and (2) the transition in the qualitative behavior of the NWFETs from rectifying to Ohmic with only a few nanometers of dopant-enriched VS overcoating.

In summary, the characteristics of NWFETs were correlated with spatial inhomogeneities in dopant atom concentrations. These results provide an illuminating example of how distinct dopant incorporation kinetics for VLS and VS growth can dramatically influence the behavior of devices on a single nanowire and between different nanowires. The agreement between the experimental data and simple models support the notion that intentional surface doping, followed by etching of the channel in a NWFET, is a viable approach to the fabrication of ohmic contacts while maintaining a good gate response.[22]

This work was supported by the National Science Foundation under the MRSEC (R.A.S.) Grant No. DMR-0520513, CAREER (D.E.P., J.L.L.) Grant No. DMR-0449933, and NIRT (E.R.H.) Grant No. 0507053 programs. We acknowledge the NUANCE and NUCAPT facilities for instrumentation and D. Isheim for useful discussions. R.A.S. acknowledges the support of a National Defense Science & Engineering Graduate Fellowship. D.E.P. acknowledges the support of a Ford Foundation Diversity fellowship. L.J.L acknowledges the support of the Sloan Foundation through a Sloan research fellowship and the Camille and Henry Dreyfus Foundation.

[1] M. Li, R. B. Bhiladvala, T. J. Morrow, J. A. Sioss, K. Lew, J. M. Redwing, C. D. Keating, and T. S. Mayer, Nat. Nanotechnol. **3**, 88 (2008).
[2] Y. Jung, S. Lee, A. T. Jennings, and R. Agarwal, Nano Lett. **8**, 2056 (2008).
[3] Y. Huang, X. Duan, Y. Cui, L. J. Lauhon, K. Kim, and C. M. Lieber, Science **294**, 1313 (2001).
[4] O. Hayden, R. Agarwal, and C. M. Lieber, Nature Mater. **5**, 352 (2006).
[5] B. Tian, X. Zheng, T. J. Kempa, Y. Fang, N. Yu, G. Yu, J. Huang, and C. M. Lieber, Nature (London) **449**, 885 (2007).
[6] Z. Fan, J. C. Ho, Z. A. Jacobson, R. Yerushalmi, R. L. Alley, H. Razavi, and A. Javey, Nano Lett. **8**, 20 (2008).
[7] A. Javey, S. W. Nam, R. S. Friedman, H. Yan, and C. M. Lieber, Nano Lett. **7**, 773 (2007).
[8] D. E. Perea, E. R. Hemesath, E. J. Schwalbach, J. L. Lensch-Falk, P. W. Voorhees, and L. J. Lauhon, Nat. Nanotechnol. **4**, 315 (2009).
[9] D. E. Perea, E. Wijaya, J. L. Lensch-Falk, E. R. Hemesath, and L. J. Lauhon, J. Solid State Chem. **181**, 1642 (2008).
[10] G. Imamura, T. Kawashima, M. Fujii, C. Nishimura, T. Saitoh, and S. Hayashi, Nano Lett. **8**, 2620 (2008).
[11] E. Tutuc, J. O. Chu, J. A. Ott, and S. Guha, Appl. Phys. Lett. **89**, 263101 (2006).
[12] Y. Wu, J. Xiang, C. Yang, W. Lu, and C. M. Lieber, Nature (London) **430**, 61 (2004).
[13] W. M. Weber, L. Geelhaar, A. P. Graham, E. Unger, G. S. Duesberg, M. Liebau, W. Pamler, C. Cheze, H. Riechert, P. Lugli, and F. Kreupl, Nano Lett. **6**, 2660 (2006).
[14] S. M. Woodruff, N. S. Dellas, B. Z. Liu, S. M. Eichfeld, T. S. Mayer, J. M. Redwing, and S. E. Mohney, J. Vac. Sci. Technol. B **26**, 1592 (2008).
[15] See EPAPS supplementary material at http://dx.doi.org/10.1063/1.3250431 E-APPLAB-95-037942 for results pertaining to additional devices and APT growth details.
[16] O. C. Hellman, J. A. Vandenbroucke, J. Rüsing, D. Isheim, and D. N. Seidman, Microsc. Microanal. **6**, 437 (2000).
[17] R. B. Fair, in *Semiconductor Materials and Process Technology Handbook*, edited by G. E. McGuire (Noyes, New Jersey, 1988), pp. 501–505.
[18] M. T. Bjork, H. Schmid, J. Knoch, H. Riel, and W. Riess, Nat. Nanotechnol. **4**, 103 (2009).
[19] K. Varahramyan and E. J. Verret, Solid-State Electron. **39**, 1601 (1996).
[20] D. M. Caughey and R. E. Thomas, Proc. IEEE **55**, 2192 (1967).
[21] D. B. M. Klaassen, Solid-State Electron. **35**, 953 (1992).
[22] J. E. Allen, E. R. Hemesath, and L. J. Lauhon, Nano Lett. **9**, 1903 (2009).